Environmental Science and Pollution Research (2020) 27:1176–1185
https://doi.org/10.1007/s11356-018-2171-3

ENVIRONMENTAL AND SUSTAINABLE CHEMICAL ENGINEERING

Boosting the catalytic activity of natural magnetite for wet peroxide oxidation

Silvia Álvarez-Torrellas[1,2] · Macarena Munoz[1] · Victor Mondejar[1] · Zahara M. de Pedro[1] · Jose A. Casas[1]

Received: 19 March 2018 / Accepted: 26 April 2018 / Published online: 2 June 2018

Abstract

This work explores the modification of naturally occurring magnetite by controlled oxidation (200–400 °C, air atmosphere) and reduction (300–600 °C, H_2 atmosphere) treatments with the aim of boosting its activity in CWPO. The resulting materials were fully characterized by XRD, XPS, TGA, TPR, SEM, and magnetization measurements, allowing to confirm the development of core-shell type structures. The magnetite core of the solid remained unchanged upon the treatment whereas the Fe(II)/Fe(III) ratio of the shell was modified (e.g. 0.42, 0.11 and 0.63 values were calculated for pristine Fe_3O_4, Fe_3O_4-O400, and Fe_3O_4-R400, respectively). The performance of the catalysts was tested in the CWPO of sulfamethoxazole (SMX) (5 mg L^{-1}) under ambient conditions and circumneutral pH ($pH_0 = 5$), using the stoichiometric dose of H_2O_2 (25 mg L^{-1}) and a catalyst load of 1 g L^{-1}. The key role of the ferrous species on the mineral shell was evidenced. Whereas the oxidation of magnetite led to significantly slower degradation rates of the pollutant, its reduction gave rise to a dramatic increase, achieving the complete removal of SMX in 1.5 h reaction time with the optimum catalyst (Fe_3O_4-R400) compared to the 3.5 h required with the pristine mineral. A reaction mechanism was proposed for SMX degradation, and a kinetic equation based on the Eley-Rideal model was accordingly developed. This model successfully fitted the experimental results. The stability of Fe_3O_4-R400 was evaluated upon five sequential runs. Finally, the versatility of the catalytic system was proved in real environmentally relevant water matrices.

Keywords Catalytic wet peroxide oxidation · H_2O_2 · Magnetite · Fe oxidation state · Sulfamethoxazole

Introduction

The removal of persistent organic pollutants during the treatment of industrial and urban wastewater is a long-standing issue of environmental relevance. In particular, over the past few years, there has been an increasing concern about the occurrence of micropollutants in the aquatic environment (Loos et al. 2013; Luo et al. 2014). They consist of a vast array of anthropogenic substances including pharmaceuticals, personal care products, hormones, and industrial chemicals. Municipal wastewater treatment plants (WWTPs) are not prepared to deal with these complex substances, and thus, most of them are not effectively removed upon the treatment (Luo et al. 2014; Petrie et al. 2015). Despite their hazardous nature and ubiquitous occurrence, they are still not regulated but this scenario is expected to change in the next few years. The European Union (EU) has recently established a watch list for 17 micropollutants monitoring in the EU water basins for their potential inclusion in the list of priority pollutants (Decision EU 2015/495). Therefore, the development of effective but also green and low-cost wastewater treatment strategies in this field is crucial.

Among the currently available technologies, catalytic wet peroxide oxidation (CWPO) is one of the most cost-effective for the treatment of low polluted wastewaters (i.e., below 15 mg L^{-1}) (Dhakshinamoorthy et al. 2012). In this system, a solid catalyst, usually based on iron (Munoz et al. 2015),

Responsible editor: Vítor Pais Vilar

Electronic supplementary material The online version of this article (https://doi.org/10.1007/s11356-018-2171-3) contains supplementary material, which is available to authorized users.

✉ Silvia Álvarez-Torrellas
satorrellas@quim.ucm.es

Macarena Munoz
macarena.munnoz@uam.es

[1] Seccion Departamental Ingenieria Quimica, Universidad Autonoma de Madrid, Ctra. Colmenar km 15, 28049 Madrid, Spain

[2] Departamento de Ingenieria Quimica, Universidad Complutense de Madrid, Av. Complutense S/N, 28040 Madrid, Spain

promotes the decomposition of H_2O_2 to hydroxyl radicals, highly reactive species which attack non-selectively most of the organic pollutants. Main efforts on the field of CWPO are being focused on the development of magnetic catalysts since they offer important advantages for the recovery and reusability of the catalyst (Munoz et al. 2015, Ribeiro et al. 2016; Han et al. 2017; Tang and Wang 2018). On the other hand, during the CWPO reaction, both Fe(II) and Fe(III) are involved in the redox cycle (Eqs. 1 and 2), being the regeneration of Fe(II) the slowest step (Duesterberg and Waite 2007):

$$\mathrm{Fe(II)} + \mathrm{H_2O_2} \rightarrow \mathrm{Fe(III)} + \mathrm{HO}\cdot + \mathrm{OH^-} \quad k = 55\ \mathrm{M^{-1}\ s^{-1}} \quad (1)$$

$$\mathrm{Fe(III)} + \mathrm{H_2O_2} \rightarrow \mathrm{Fe(II)} + \mathrm{HOO}\cdot + \mathrm{H^+} \quad k = 2 \times 10^{-3}\ \mathrm{M^{-1}\ s^{-1}} \quad (2)$$

Thus, the presence of both Fe(II) and Fe(III) species in the magnetic catalysts allows improving dramatically the production rate of hydroxyl radicals compared to conventional catalysts where only Fe(III) species is present (Munoz et al. 2013).

Magnetic nanoparticles (MNPs) represent so far the main field of study (Dhakshinamoorthy et al. 2012; Munoz et al. 2015). Nevertheless, direct application of unsupported MNPs for wastewater treatment is highly restricted. Main problems are the aggregation and consequent reduction of dispersibility, as well as their loss during supernatants discharge (Zhang et al. 2009; Zubir et al. 2014). Apart from economic reasons, it also represents an environmental concern as nanoparticles can cause toxic effects in living organisms and act as pollutant carriers (Luoma et al. 2014; Tang and Lo 2013). The immobilization of MNPs onto a suitable support would allow to overcome those drawbacks. In this sense, increasingly complex catalysts such as MNPs supported on graphene (Zubir et al. 2014) or multi-walled carbon nanotubes (Cleveland et al. 2014) have been recently developed and proved to be effective in this process but stability, economic, and environmental issues prevent their application. In this context, naturally occurring magnetic minerals appear as potentially promising catalysts given their huge availability at much lower cost than synthetic materials as well as their environmentally-friendly character (Pereira et al. 2012; Munoz et al. 2015; Pouran et al. 2014). Ilmenite ($FeTiO_3$), maghemite (γ-Fe_2O_3), green rusts ($Fe(III)_xFe(II)_y(OH)_{3x+2y-z}(A^-)_z$; $A^- = Cl^-$; ½ SO_4^{2-}) and magnetite (Fe_3O_4) have been already investigated as CWPO catalysts (García-Muñoz et al. 2017, Matta et al. 2008a, 2008b, Pouran et al. 2014, Souza et al. 2009), showing a significantly higher catalytic activity than non-magnetic ferric minerals (Matta et al. 2008b). According to a number of works (Hanna et al. 2008, Matta et al. 2007, Munoz et al. 2017a, b, Pouran et al. 2014), magnetite has been recognized as the highest active mineral in this process, showing also a suitable reusability.

In a previous work, we explored the application of natural magnetite as CWPO catalyst for the removal of the highly persistent antibiotic sulfamethoxazole (SMX) (Munoz et al. 2017a, b). The process was effective but relatively low oxidation rates were observed, requiring up to 3.5-h reaction time to reach the complete removal of the pollutant under ambient temperature and circumneutral pH. It is clear that a boost in the activity of the mineral is required for its potential application as a tertiary treatment in WWTPs. In this work, we tackle this ambitious challenge by the modification of magnetite upon controlled thermal treatments in order to produce novel core-shell materials with strong magnetic properties and enhanced catalytic activity while maintaining a reasonable stability. The developed core-shell catalysts have been fully characterized and tested in the CWPO of SMX to learn on the role of the surface Fe species on the catalytic activity and stability of the mineral. A kinetic equation based on the Eley-Rideal model has been developed to describe SMX degradation. The stability and reusability of the optimum catalyst have been investigated upon its sequential use in five consecutive runs. To further demonstrate the applicability of the catalytic system, it has been also tested in real environmentally relevant water matrices such as surface water, WWTP effluent, and hospital wastewater.

Materials and methods

Chemicals

Sulfamethoxazole (> 99%), hydrogen peroxide solution (30% wt.), nitric acid (65%), and acetic acid (> 99%) were purchased from Sigma-Aldrich. Sodium hydroxide (> 98%) was supplied by Panreac and titanium oxysulfate (> 99%) and acetonitrile (99.8%) by Fluka and Scharlau, respectively. All these chemicals of analytical grade were used without further purification. Unless otherwise indicated, deionized water was the matrix used to perform the CWPO experiments.

Modification and characterization of the catalysts

The core-shell materials were prepared by submitting the naturally occurring magnetite to controlled oxidation and reduction thermal treatments. The oxidation treatments were carried out in air atmosphere for 3 h in an oven within the temperature range of 200 to 400 °C using a heating ramp of 10 °C min^{-1}. The reduction treatments were accomplished under a diluted H_2 flow (250 N mL min^{-1} of 25 vol.% H_2 in N_2) for 3 h in a tubular quartz glass reactor with an inner diameter of 1 cm. This treatment was investigated within the temperature range of 300 to 600 °C using a heating ramp of 10 °C min^{-1}. The resulting catalysts were denoted as Fe_3O_4-XY, X: oxidation (O) or reduction (R), Y: temperature (°C).

The composition of pristine magnetite was determined by total reflection X-ray fluorescence (TXRF) using a TXRF spectrometer 8030c. Its textural properties were characterized from nitrogen adsorption-desorption isotherms at − 196 °C using a Micromeritics Tristar 3020 apparatus. Thermogravimetric analysis (TGA) was conducted in a TGA Q500 (TA Instruments) thermogravimetric analyzer under air atmosphere at a heating rate of 10 °C min^{-1}, from 30 to 900 °C. Temperature programmed reduction (TPR) was performed using a Micromeritics Chemisorb 2750 automated system under H_2 atmosphere (5 vol.% H_2 in Ar) using the same heating ramp conditions as TGA analysis.

The composition of the material surface was explored by X-ray photoelectron spectrometry (XPS) with a Termo Scientific K-Alpha apparatus equipped with a Kα X-ray excitation source, 1486.68 eV. The software "XPS-Peak 4.1" was used for spectrograms deconvolution. The magnetic properties of the solids were determined with a Quantum Design MPMS XL-5 superconducting quantum interference device (SQUID). The magnetic moment (M) was measured as a function of the applied field (H) at room temperature. The crystalline phases in the pristine and modified minerals were analyzed by X-Ray diffraction (XRD) using a Siemens model D-5000 diffractometer with Cu Kα radiation. Scanning electron microscopy (SEM) images of representative samples were obtained using a Philips XL30 microscope.

CWPO experiments

Oxidation runs were carried out in a glass batch reactor (500 mL), equipped with a stirrer (700 rpm) and temperature control. The operating conditions were established according to a previous contribution where the effect of pH_0, temperature, H_2O_2 dose, and magnetite concentration was investigated (Munoz et al. 2017a, b). In this sense, a circumneutral pH_0 value ($pH_0 = 5$), ambient temperature (25 °C), the stoichiometric amount of H_2O_2 for complete mineralization of SMX, and a catalyst load of 1 g L^{-1} were selected. The initial concentration of SMX was fixed at 5 mg L^{-1}.

The performance of the optimum catalyst was also investigated in real environmentally relevant water matrices where SMX usually appears: WWTP effluent, surface water, and hospital wastewater. All the experiments were carried out in triplicate being the standard deviation lower than 5% in all cases.

Analytical methods

Liquid samples were periodically taken along reaction and immediately analyzed. The catalyst was previously separated by filtration using a PTFE filter (pore size 0.45 μm). SMX and the aromatic reaction intermediates were followed by high-performance liquid chromatography, HPLC-UV (Varian, Mod. ProStar) using an Eclipse Plus C18 column (15 cm length, 4.6 mm diameter) (Agilent). The analyses were carried out at 270 nm using a 25/75% (*v*/*v*) mixture of acetonitrile and acetic acid aqueous solution (75 mM) as the mobile phase. H_2O_2 and leached iron concentrations were determined by colorimetric titration with a UV 2100 Shimadzu UV-VIS spectrophotometer using the titanium sulfate (Eisenberg 1943) and the *o*-phenantroline (Sandell 1959) methods, respectively.

Results and discussion

Catalysts characterization

The pristine mineral was fully characterized in a previous work (Munoz et al. 2017a, b). Briefly, the iron content was close to the theoretical one for pure Fe_3O_4 (73% wt); its surface area value was relatively low (7.5 m^2 g^{-1}), which is usual for iron minerals (Costa et al. 2008; He et al. 2015), and the particles appeared mostly spherical, with an average size of 203 nm.

The catalysts were prepared by controlled thermal oxidation or reduction of the starting Fe_3O_4. In first place, the TGA and TPR profiles of the pristine mineral in the range of 30–1000 °C under air and H_2 atmosphere, respectively, were investigated (Fig. 1). The TGA profile showed a weight gain from 200 to 400 °C, which can be attributed to the partial oxidation of the particle surface from magnetite to maghemite according to the process (Pereira et al. 2012; Oliveira et al. 2004):

$$Fe_3O_4 + \frac{1}{4}\,O_2 \rightarrow \frac{3}{2}\,\gamma\text{–}Fe_2O_3 \quad (3)$$

As can be seen in the TPR profile, the reduction of the sample occurred in the temperature range of 300–600 °C, with a peak centered at 512 °C. This peak corresponded to the reduction of magnetite to wüstite and finally to metallic iron according to Eqs. 4 and 5, respectively (Costa et al. 2008; Tiernan et al. 2001):

$$Fe_3O_4 + H_2 \rightarrow 3FeO + H_2O \quad (4)$$

$$FeO + H_2 \rightarrow Fe^0 + H_2O \quad (5)$$

On the basis of the TGA and TPR results, the oxidation treatment of Fe_3O_4 was carried out at 200, 300, and 400 °C; and its reduction was conducted at 300, 400, 500, and 600 °C. The obtained materials were characterized by XPS and magnetization measurements to learn on the kind of Fe species present in the mineral surface as well as the magnetic properties of the solids. These results are summarized in Table 1. The deconvolution of the Fe 3p core-level spectra of the pristine,

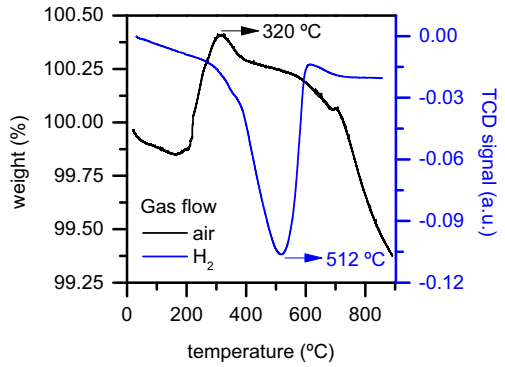

Fig. 1 TPO and TPR profiles of pristine Fe_3O_4

oxidized and reduced mineral at different temperatures can be seen in Fig. S1 of the Supplementary Material, while their magnetization hysteresis loops are collected in Fig. 2.

The deconvolution of the XPS profiles showed the presence of both Fe(II) and Fe(III) species in all the materials (Yamashita and Hayes 2008). The Fe(II)/Fe(III) ratio calculated for the raw mineral was 0.42, close to the theoretical stoichiometric one of magnetite (Yamashita and Hayes 2008). The oxidation of the solid led to a gradual increase of the Fe(III) proportion at the mineral surface, reaching a Fe(II)/Fe(III) ratio of only 0.11 with the highest temperature tested (400 °C). Accordingly, the color of the material evolved from dark brown to intense orange with increasing the oxidation temperature (see Fig. S2 of the Supplementary Material for the illustrations). In the same line, the magnetization saturation value (M_S) as well as the coercivity (H_C) and saturation remanence (M_R) of the mineral were progressively decreased (Table 1, Fig. 2). Nevertheless, it should be highlighted that the loss of magnetization was 16% at the most, and thus, the separation of the solid from water by the application of a magnetic field was warranted for all the oxidized samples. It could be then assumed that the core of the solid remained unchanged after the oxidation treatment. To corroborate this hypothesis, the highly oxidized sample, Fe_3O_4-O400, was further characterized by XRD (Fig. 3). Magnetite was the main phase in the XRD pattern but the presence of maghemite (γ-Fe_2O_3) was also confirmed. The latter phase can only be distinguished from the former one by the appearance of two extra peaks at 23.77° and 26.10° (Kim et al. 2012), which, although being of low significance, were clearly distinguished in the oxidized sample. According to these results, it can be concluded that the oxidation of magnetite under these operating conditions allowed to modify the iron species at the mineral surface while maintaining its crystalline structure and magnetic properties almost unchanged, giving rise to a core-shell structure type.

In contrast to the oxidation treatment, the reduction process led to a significant increase in the Fe(II)/Fe(III) ratio up to 0.87 at 600 °C (Table 1), evolving the color of the material to black (see Fig. S2 of the Supplementary Material for the illustrations). As a result, a slight growth in the magnetization of the material was observed with increasing the reduction temperature (Table 1, Fig. 2), which is consistent with a previous work (Costa et al. 2008). It can be explained by the formation of metallic iron at the mineral surface, whose magnetic properties are well-known to be much higher than those of pure magnetite (Vecchia et al. 2008). The formation of metallic iron took place above 500 °C, where the increase of the magnetization of the material was more evident. Both Fe_3O_4-R400 and Fe_3O_4-R600 samples were further characterized by XRD to gain further insights on the possible changes in the mineral structure upon its reduction (Fig. 3). While the former did not suffer any significant alteration, corresponding entirely to the magnetite phase, the XRD pattern of the latter showed clear peaks corresponding to both FeO and Fe^0 species, apart from those corresponding to magnetite (Costa et al. 2008). In any case, magnetite was the main iron oxide in the samples, being the modified minerals of core-shell type, in line with the results obtained by its oxidation. It must be noted that the morphology and size of magnetite particles were not significantly affected by either the oxidation or reduction treatments (see Fig. S3 of the Supplementary Material for SEM images).

Table 1 Characterization of the core-shell magnetic catalysts

Catalyst	Thermal treatment		Fe(II)/Fe(III) ratio	M_S (emu g^{-1})	H_C (Oe)	M_R (emu g^{-1})
	Treatment	Temperature (°C)				
Pristine Fe_3O_4	–	–	0.42	77.8	87.5	7.8
Fe_3O_4-O200	Oxidation (air atmosphere)	200	0.23	74.5	80.8	7.3
Fe_3O_4-O300		300	0.15	71.1	74.5	7.1
Fe_3O_4-O400		400	0.11	65.3	74.2	7.1
Fe_3O_4-R300	Reduction (H_2 flow)	300	0.56	78.4	78.0	7.9
Fe_3O_4-R400		400	0.63	81.5	78.5	8.2
Fe_3O_4-R500		500	0.78	82.0	80.6	7.3
Fe_3O_4-R600		600	0.87	84.4	84.2	7.4

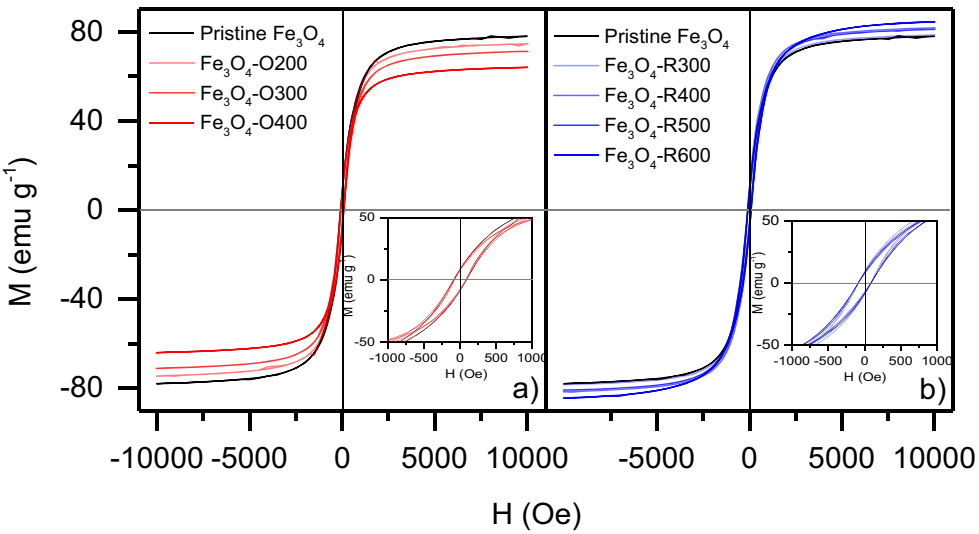

Fig. 2 Magnetization hysteresis loop of oxidized (**a**) and reduced (**b**) magnetite at different temperatures. The insets show the details of the cycles in the field range—1000 to 1000 Oe

Influence of the thermal treatment of magnetite on its catalytic activity

The developed core-shell materials were used as catalysts in the CWPO of SMX under ambient temperature and circumneutral pH ($pH_0 = 5$). Previously, blank experiments in the absence of oxidant or catalyst were carried out to distinguish their contribution to the reaction. Adsorption of SMX onto the solids was not significant, as its concentration hardly decreased (< 5%) in the absence of H_2O_2 after 4 h. On the other hand, the key role of the catalyst in the process was demonstrated in the experiment performed without its addition, where only 1% of SMX was degraded within 4 h.

Oxidation treatment

The impact of the oxidation treatment of magnetite on its catalytic activity on the CWPO of SMX can be seen in Fig. 4a. As observed, the oxidation of the mineral at increasing temperatures led to a progressive decrease on the degradation rate of the pollutant. Accordingly, the consumption of H_2O_2 was reduced from 50% with the pristine mineral to only 10% with the highly oxidized catalyst (Fe_3O_4-O400). These results are consistent with the decrease on the proportion of Fe(II) species on the solid surface (Costa et al. 2008; Dhakshinamoorthy et al. 2012). Thus, the oxidation of the mineral can be discarded as an effective treatment to boost the activity of the magnetite. With regard to the stability of the oxidized materials, the Fe leaching was slightly lower than that observed with the pristine mineral (0.3 vs. 0.5 mg L^{-1}).

The oxidation pathway of SMX upon CWPO catalyzed by magnetite was described in detail in our previous contribution (Munoz et al. 2017a, b). Briefly, SMX was hydroxylated in the first place leading to the formation of two aromatic intermediates, one of them produced by the addition of the hydroxyl group to the aromatic ring and the other by the replacement of a substituent by the hydroxyl group in the drug structure. Further attack of hydroxyl radicals led to the breaking down of these species in smaller fragments, giving rise finally to non-toxic short chain organic acids. The aromatic intermediates formed along reaction were also followed in the current work (see Fig. S4 of the Supplementary Material for their tentative molecular structures as well as their evolution upon reaction with the oxidized minerals). Consistent with the low conversion of SMX, the amount of aromatic intermediates gradually increased with reaction time, not being observed their degradation along the process under these conditions. In the same line, the pH of the reaction medium was slightly decreased from pH_0 5 to values in the range 4.0–4.5 after 4 h reaction time due to the formation of short-chain organic acids (Munoz et al. 2017a, b).

Reduction treatment

The results obtained in the CWPO of SMX with the reduced minerals at different temperatures are depicted in Fig. 4b. It can be clearly seen that the reduction of magnetite led to a significant increase on the oxidation rate of the pollutant. Whereas 3.5 h were required to achieve the complete degradation of the drug with the pristine mineral; 1.5 h was enough to reach its total conversion using the optimum material (Fe_3O_4-R400). These results allow to confirm that the Fe(II) species produced along the reduction treatment plays a key role on the oxidation process since this species is the main responsible for HO generation. The small decrease on the catalytic activity of the mineral with increasing reduction temperature from 400 to 500 °C could be related to the presence of wüstite and zero-valent Fe species, in accordance with a previous work (Costa et al. 2008). The decomposition of H_2O_2 was increased up to 70% at the end of the reaction (90 min)

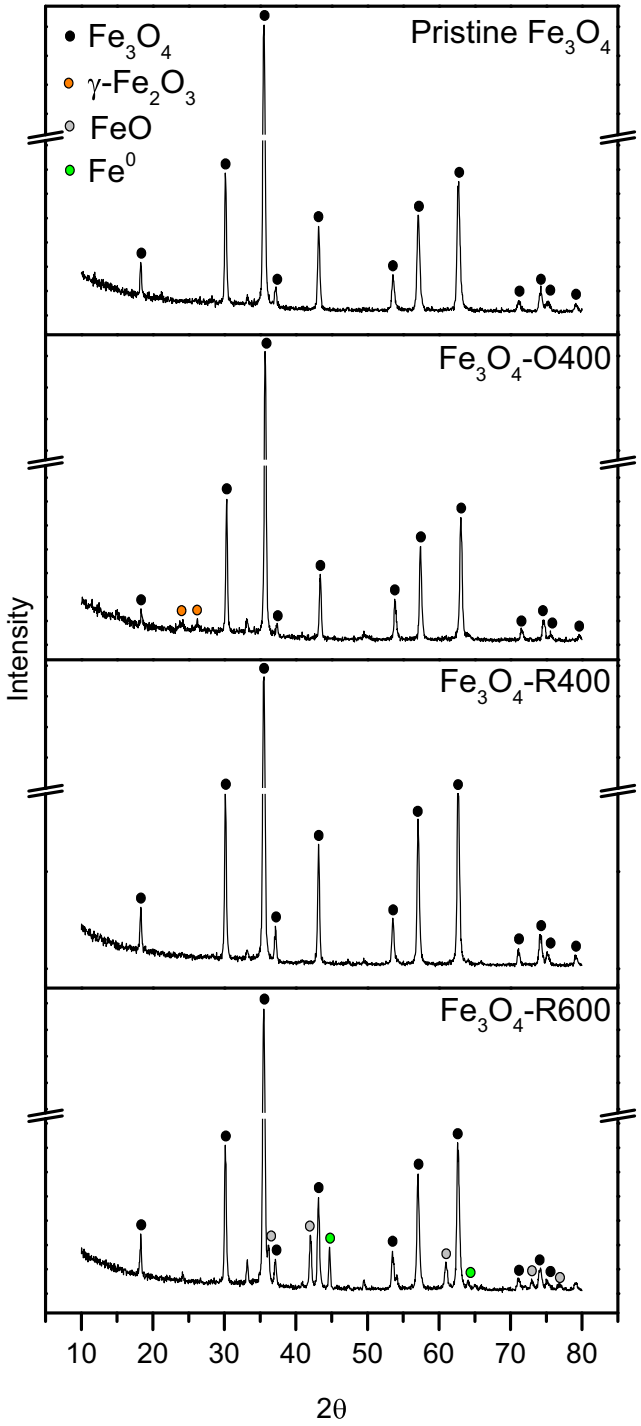

Fig. 3 XRD patterns of the pristine, oxidized, and reduced mineral at different temperatures. Major peaks are identified using ICDD PDFs 00-039-1346 (γ-Fe_2O_3), 01-080-6402 (Fe_3O_4), 00-006-0696 (Fe^0) and 00-006-0615 (FeO)

with the optimum catalyst, and the aromatic intermediates were completely removed along the reaction with all the reduced samples (see Fig. S4 of the Supplementary Material for their evolution upon reaction). Accordingly, the pH of the reaction medium was reduced up to 3.5 at the end of the reaction, which can be related to the formation of short-chain organic acids as final reaction products (Munoz et al. 2017a, b).

It must be noted that iron leaching from the materials reduced up to 500 °C was very similar to that observed for pristine magnetite (~ 0.4 mg L^{-1}), and thus, the reduction treatment of the mineral allowed to boost its activity while maintaining its suitable stability. In any case, to determine the contribution of the homogeneous Fenton reaction to the removal of SMX, an additional experiment was conducted under the same operating conditions using dissolved iron as catalyst (0.5 mg L^{-1} Fe^{2+}). Remarkably, SMX removal was below 15% after 90 min, whereas complete degradation of the drug was achieved using the optimum catalyst (Fe_3O_4-R400) at the same reaction time, confirming the key role of the solid catalyst in the process (see Fig. S5 of the Supplementary Material for experimental data). Nevertheless, reduction at temperatures above 500 °C was counterproductive from the stability point of view, since the mineral reduced at 600 °C (Fe_3O_4-R600) suffered strong Fe leaching (6 mg L^{-1}). These results can be explained by the presence of important amounts of zero-valent iron on the shell of this highly reduced material. It is well-known that zero-valent iron is more prone to leach than iron oxides, leading in practice to a homogeneous Fenton reaction (Xu and Wang 2011). For this reason, this material was not further evaluated in this study.

Kinetic model

The reaction mechanism proposed for the CWPO of SMX by the magnetic core-shell materials developed in this work is based on the Eley-Rideal type mechanism. We have only focused on the degradation of SMX and thus, not all the reactions taking place towards its complete mineralization have been considered. It must be noted that SMX was in its neutral form under the operating conditions tested in this work. This compound undergoes two acid-base processes, showing two pK_a values ($pK_{a,1}$ = 1.6, $pK_{a,2}$ = 5.7) (Boreen et al. 2004). The initial pH of the reaction medium was adjusted to 5, being the final values within the range of 3.5–4.5 at the end of the reactions. On the other hand, as has been confirmed by the characterization of the materials, both Fe(II) and Fe(III) species are present at the catalyst surface. It has been also demonstrated that the increase of Fe(II)/Fe(III) ratio led to a faster degradation of SMX, suggesting that Fe(II) species plays a key role as active center. In addition, when Fe(II) was reduced to metallic iron (samples reduced above 400 °C), the reaction rate also decreased. Briefly, the proposed reaction mechanism started by the adsorption of a SMX molecule onto a free active site (Fe(II)) of the catalyst, giving rise to Fe(II)-SMX (Eq. 6). This adsorbed compound reacts with a free hydroxyl radical from the bulk reaction medium leading to the formation of an oxidation product (OP) (Eq. 7). In a next step, OP is released

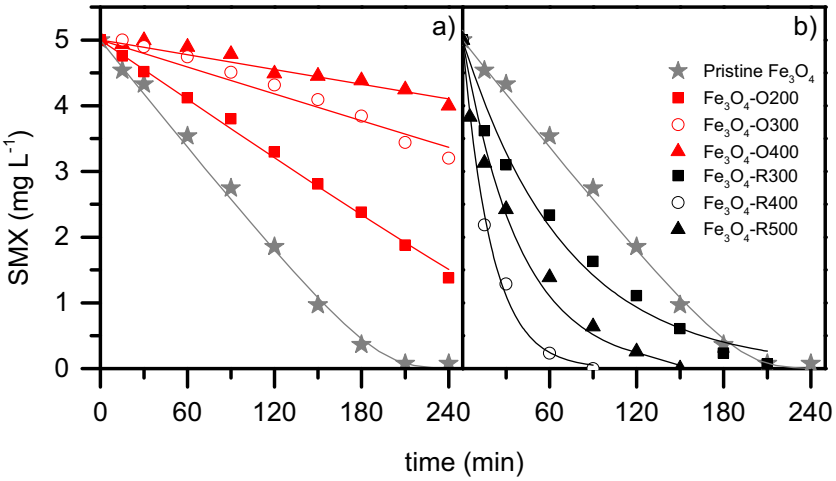

Fig. 4 Effect of the oxidation (**a**) and reduction (**b**) treatment of magnetite on its catalytic activity in the CWPO of SMX ($[SMX]_0$ = 5 mg L^{-1}; $[H_2O_2]_0$ = 25 mg L^{-1}; [catalyst] = 1 g L^{-1}; pH_0 = 5; T = 25 °C). Experimental data (symbols) and model fit (solid lines)

from the catalyst, becoming the active site Fe(II) newly available (Eq. 8). Additionally, as shown in the introduction section, part of the production of hydroxyl radicals takes place by the reduction of H_2O_2 onto free Fe(II) species, oxidizing it to Fe(III) species, and releasing the hydroxyl radical and a hydroxyl ion (Eqs. 1 and 2).

$$\mathrm{Fe(II)} + \mathrm{SMX} \leftrightarrow \mathrm{Fe(II)-SMX} \tag{6}$$

$$\mathrm{Fe(II)-SMX} + \mathrm{HO}\cdot \leftrightarrow \mathrm{Fe(II)-OP} \tag{7}$$

$$\mathrm{Fe(III)-OP} \rightarrow \mathrm{Fe(II)} + \mathrm{OP} + \mathrm{H^+} \tag{8}$$

The release of the oxidation product is assumed the slowest step and thus, the rate-limiting one. Additionally, under these operating conditions, it can be assumed that the concentration of hydroxyl radicals remains practically constant as H_2O_2 is in excess for SMX degradation, and thus, it can be included in a lumped kinetic constant. Taking into account all these considerations, the net oxidation rate of SMX can be expressed by the following kinetic equation:

$$(-r_{SMX}) = -\frac{dC_{SMX}}{dt} = \frac{k_1 \times C_{HO} \times C_{SMX}}{1 + K_2 \times C_{SMX}} = \frac{k_1 \times C_{SMX}}{1 + K_2 \times C_{SMX}} \tag{9}$$

where C_{SMX} is the concentration of SMX (mg L^{-1}); k_1 is a lumped kinetic constant (min^{-1}) and K_2 is another lumped constant including kinetics and adsorption constants (L mg^{-1}).

The software package Scientist 3.0 (Micromath®) was used to solve the Eq. 9 and fit the experimental data. The fitting curves obtained were in fairly good agreement with the experimental data obtained with all the materials developed in this work (Fig. 4). The values of the rate constants and the correlation coefficients are collected in Table 2. It is clear that the thermal treatments of the mineral showed an important effect on the kinetics of the process. The degradation of SMX catalyzed by the pristine and the oxidized materials responds to a linear tendency with reaction time, suggesting an apparent zero-order kinetics, which is consistent with previous works (He et al. 2015; Munoz et al. 2017a, b). In these cases, the high value of the global parameter K_2 allows to simplify the kinetic equation and the values of k_1/K_2 ratio could be used to compare the activity of the catalysts. Consistent with the aforementioned discussion of the experimental results, the oxidation of magnetite led to significantly slower degradation rates, up to 1 order of magnitude lower at the highest oxidation temperature tested (400 °C) due to the predominant presence of Fe(III) species. On the other hand, the thermal reduction of the mineral allowed to increase dramatically the oxidation rate of SMX. In this case, the global parameter K_2 was almost negligible, and thus, the degradation of SMX can be described by pseudo-first order kinetics being the kinetic constant (k_1), the parameter used to compare the catalysts activity. It is clear that the increasingly higher amounts of Fe(II) species available at the catalyst surface of reduced samples allowed to increase dramatically the oxidation rate of SMX due to the increase generation of hydroxyl radicals. As explained above, Fe_3O_4-R400 was the optimum catalyst for this process.

Table 2 Values of the rate constants ($[SMX]_0$ = 5 mg L^{-1}; $[H_2O_2]_0$ = 25 mg L^{-1}; [catalyst] = 1 g L^{-1}; pH_0 = 5; T = 25 °C)

Catalyst	$k_1 \times 10^2$ (min^{-1})	K_2 (L mg^{-1})	k_1/K_2 (mg L^{-1} min^{-1})	R^2
Pristine Fe_3O_4	10.25	3.53	0.029	0.9988
Fe_3O_4-O200	5.55	3.42	0.016	0.9996
Fe_3O_4-O300	3.70	5.28	0.007	0.9992
Fe_3O_4-O400	2.11	5.46	0.004	0.9997
Fe_3O_4-R300	1.40	8.12×10^{-16}	–	0.9931
Fe_3O_4-R400	5.02	1.81×10^{-16}	–	0.9980
Fe_3O_4-R500	2.52	2.05×10^{-16}	–	0.9908

Stability tests

The reusability of the optimum catalyst (Fe_3O_4-R400) was evaluated by its use upon five sequential runs. The catalyst was recovered by magnetic separation and dried at low temperature (60 °C) overnight after each trial. The obtained results are depicted in Fig. 5. It is clear that the catalyst suffered a slight deactivation upon its sequential application along the first three uses, being required an additional period of 0.5 h in the subsequent use to achieve the complete removal of the drug. In the following runs, the catalyst maintained its activity unchanged, reaching the same results as those obtained with the pristine mineral. This is consistent with the high stability of magnetite under these operating conditions (Munoz et al. 2017a, b).

The deactivation of the catalyst cannot be explained by the leaching of iron since it was around 0.4 mg L^{-1} upon each application. On the other hand, the presence of carbonaceous deposits was of low significance since the carbon content of the used catalyst was very low (0.1% wt) while the BET surface remained unchanged (7.0 m^2 g^{-1}). Remarkably, the magnetic properties of the solid were not affected by its use (see Fig. S6 of the Supplementary Material for the magnetization hysteresis loops of the catalyst after each sequential run). Main reason for deactivation must be then related to the partial oxidation of the catalyst surface during the reaction. In fact, the Fe(II)/Fe(III) ratio was decreased upon sequential uses, reaching a value of 0.43 after the third run, almost the same of the prisitine mineral (see Fig. S7 of the Supplementary Material for the deconvolution of the Fe 3p core-level spectrum of the used catalyst). These results are in agreement with the proposed reaction mechanism. The presence of progressively lower amounts of Fe(II) species led to a decay of the available active sites for SMX adsorption. At the same time, it apparently resulted in a slower production of hydroxyl radicals, necessary for the oxidation of the adsorbed SMX species. Consistent with this, H_2O_2 conversion along the subsequent runs was slower, being the consumption gradually decreased from 70 to 45% from the first to the third run.

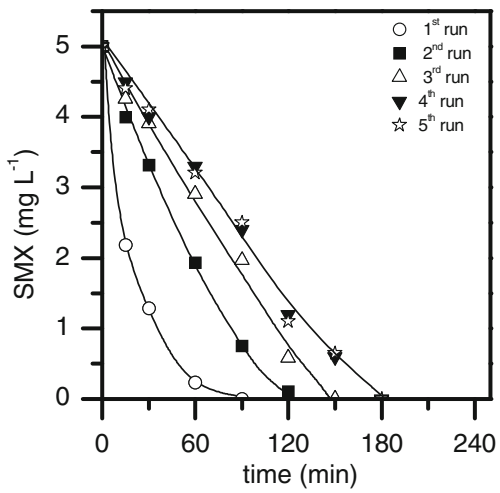

Fig. 5 Stability of Fe_3O_4-R400 upon SMX oxidation in five sequential runs ($[SMX]_0 = 5$ mg L^{-1}; $[H_2O_2]_0 = 25$ mg L^{-1}; [catalyst] = 1 g L^{-1}; $pH_0 = 5$; $T = 25$ °C)

Operation in environmentally relevant water matrices

As a proof of concept, the optimum catalyst (Fe_3O_4-R400) was used in different environmentally relevant water matrices doped with SMX (5 mg L^{-1}). A WWTP effluent, a surface water sample, and a real hospital wastewater were selected for such goal (Luo et al. 2014; Verlicchi et al. 2010). The characterization of these aqueous matrices is provided in the Table S1 of the Supplementary Material. Briefly, the conductivity values of the WWTP effluent, the surface water, and the hospital wastewater were 462, 200, and 1185 μS cm^{-1}, respectively. Regarding the organic content, the hospital wastewater was the most polluted effluent with a high TOC value (110 mg L^{-1}) whereas the WWTP effluent and surface water showed very low TOC contents (2.6–2.7 mg L^{-1}). As can be seen, the composition of the real aqueous solutions was strongly different, and thus, direct comparison among them is not straightforward. Nevertheless, these trials allow to prove if the process is effective in different water media.

The oxidation of SMX in the aforementioned water matrices is depicted in Fig. 6. As can be seen, the degradation of the drug was not significantly affected by the water matrix composition, with the exception of the highly complex hospital wastewater. In this sense, complete removal of the drug was achieved in 1.5 and 2 h reaction time within the surface water and WWTP effluent, respectively, whereas 70% removal of the pharmaceutical was achieved in 4 h reaction time using the

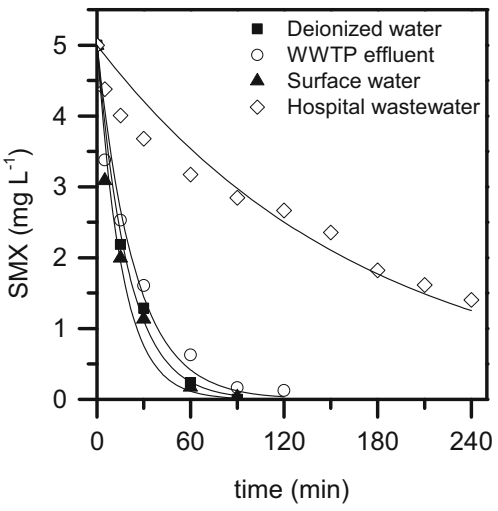

Fig. 6 Evolution of SMX upon CWPO with Fe_3O_4-R400 in different real aqueous matrices ($[SMX]_0 = 5$ mg L^{-1}; $[H_2O_2]_0 = 25$ mg L^{-1}; [catalyst] = 1 g L^{-1}; $pH_0 = 5$; $T = 25$ °C). Experimental (symbols) and model fit (solid lines)

hospital wastewater. The obtained rate constants (k_1) for the degradation of SMX were 6.29×10^{-2} ($R^2 = 0.988$), 4.14×10^{-2} ($R^2 = 0.984$), and 0.58×10^{-2} min^{-1} ($R^2 = 0.990$) in surface water, WWTP effluent, and hospital wastewater, respectively. The characterization of the used catalysts and the oxidation effluents revealed that they were not significantly modified as a consequence of the water matrix (Fe leached < 0.4 mg L^{-1}; carbonaceous deposits < 0.1% wt). Remarkably, the magnetic properties of the catalyst remained unchanged after reaction (see Fig. S6 of the Supplementary Material for the magnetization hysteresis loops of the used catalysts). Therefore, the inhibition effect observed with the hospital wastewater seems to be related to the scavenging of hydroxyl radicals due to the co-existing substances present in the aqueous matrices, in particular, salts, as well as to their consumption by other organic species.

The results achieved in the current work significantly improved those reached in our previous contribution where the pristine mineral was used under the same operating conditions (Munoz et al. 2017a, b). In that case, up to 5 and 5.5 h were required to achieve the complete removal of SMX in surface water and WWTP effluent, respectively, whereas only 30% of SMX degradation was reached in 4-h reaction time within the same hospital wastewater matrix.

Conclusions

It has been proved that the modification of naturally occurring magnetite by controlled thermal treatments results in novel core-shell materials with strong magnetic properties and tuned Fe(II)/Fe(III) ratios on the surface. The latter has shown to be crucial on the activity of the resulting catalyst. Whereas the oxidation of magnetite led to sluggish kinetics due to the presence of increasing amounts of ferric species; its reduction gave rise to extremely high SMX degradation rates due to the high proportion of ferrous species. The reduction temperature of 400 °C was found to be the optimum for the development of a highly active catalyst with a reasonable stability. Higher reduction temperatures led to the formation of zero-valent iron species, resulting in poor stability due to strong Fe leaching.

The applicability of the optimum catalyst (Fe_3O_4-R400) was demonstrated not only in deionized water but in real environmentally relevant water matrices where micropollutants are usually present like surface water, WWTP effluent, and hospital wastewater. Remarkably, the performance of the catalyst was very similar regardless of the composition of the aqueous matrix with the exception of the complex hospital wastewater, which led to a partial inhibition of the reaction due to scavenging effects given the presence of important amounts of salts and organic content. These findings offer new perspectives for the design and optimization of active, easily-recoverable, and durable catalysts for CWPO. In particular, the catalytic system developed in this work represents an interesting alternative as tertiary treatment in WWTPs or even as a purification step in drinking-water-treatment plants.

Acknowledgments Authors would like to acknowledge the use of Servicio General de Apoyo a la Investigación-SAI, Universidad de Zaragoza.

Funding information This research has been supported by the Spanish MINECO through the project CTM2016-76454-R and by the CM through the project S2013/MAE-2716. S. Alvarez-Torellas and M. Munoz thank the Spanish MINECO for the Juan de la Cierva-Formación (FJCI-2014-19916) and Juan de la Cierva-Incorporación (IJCI-2014-19427) postdoctoral contracts, respectively.

References

Boreen AL, Arnold WA, McNeill K (2004) Photochemical fate of sulfa drugs in the aquatic environment: sulfa drugs containing five-membered heterocyclic groups. Environ Sci Technol 38:3933–3940

Cleveland V, Bingham J, Kan E (2014) Heterogeneous Fenton degradation of bisphenol a by carbon nanotube-supported Fe_3O_4. Sep Purif Technol 133:388–395

Costa RCC, Moura FCC, Ardisson JD, Fabris JD, Lago RM (2008) Highly active heterogeneous Fenton-like systems based on Fe0/Fe3O4 composites prepared by controlled reduction of iron oxides. Appl Catal B 83:131–139

Decision (EU) 2015/495 of 20 March 2015 establishing a watch list of substances for Union-wide monitoring in the field of water policy pursuant to Directive 2008/105/EC of the European Parliament and of the Council

Dhakshinamoorthy A, Navalon S, Alvaro M, Garcia H (2012) Metal nanoparticles as heterogeneous Fenton catalysts. ChemSusChem 5:46–64

Duesterberg CK, Waite TD (2007) Kinetic modeling of the oxidation of p-hydroxybenzoic acid by Fenton's reagent: implications of the role of quinones in the redox cycling of iron. Environ Sci Technol 41:4103–4110

Eisenberg GM (1943) Colorimetric determination of hydrogen peroxide. Ind Eng Chem Res 15:327–328

García-Muñoz P, Pliego G, Zazo JA, Barbero B, Bahamonde A, Casas JA (2017) Modified ilmenite as catalyst for CWPO-photoassisted process under LED light. Chem Eng J 318:89–94

Han S, Yu H, Yang T, Wang S, Wang X (2017) Magnetic activated-ATP@Fe_3O_4 nanocomposite as an efficient Fenton-like heterogeneous catalyst for degradation of ethidium bromide. Sci Rep 7:1–12

Hanna K, Kone T, Medjahdi G (2008) Synthesis of the mixed oxides of iron and quartz and their catalytic activities for the Fenton-like oxidation. Catal Commun 9:955–959

He H, Zhong Y, Liang X, Tan W, Zhu J, Yan Wang C (2015) Natural magnetite: an efficient catalyst for the degradation of organic contaminant. Sci Rep 5:1–10

Kim W, Suh C, Cho S, Roh K, Kwon H, Song K, Shon I (2012) A new method for the identification and quantification of magnetite–maghemite mixture using conventional X-ray diffraction technique. Talanta 94:348–352

Loos R, Carvalho R, António DC, Comero S, Locoro G, Tavazzi S, Paracchini B, Ghiani M, Lettieri T, Blaha L, Jarosova B, Voorspoels S, Servaes K, Haglund P, Fick J, Lindberg RH, Schwesig D, Gawlik BM (2013) EU-wide monitoring survey on

emerging polar organic contaminants in wastewater treatment plant effluents. Water Res 47:6475–6487

Luo Y, Guo W, Ngo HH, Nghiem LD, Hai FI, Zhang J, Liang S, Wang XC (2014) A review on the occurrence of micropollutants in the aquatic environment and their fate and removal during wastewater treatment. Sci Total Environ 473–474:619–641

Luoma SN, Khan FR, Croteau M (2014) Chapter 5—bioavailability and bioaccumulation of metal-based engineered nanomaterials in aquatic environments: concepts and processes. Front Nanosci 7:157–193

Matta R, Hanna K, Chiron S (2007) Fenton-like oxidation of 2,4,6-trinitrotoluene using different iron minerals. Sci Total Environ 385:242–251

Matta R, Hanna K, Chiron S (2008a) Oxidation of phenol by green rust and hydrogen peroxide at neutral pH. Sep Purif Technol 61:442–458

Matta R, Hanna K, Kone T, Chiron S (2008b) Oxidation of 2,4,6-trinitrotoluene in the presence of different iron-bearing minerals at neutral pH. Chem Eng J 144:453–458

Munoz M, de Pedro ZM, Menendez N, Casas JA, Rodriguez JJ (2013) A ferromagnetic-alumina-supported iron catalyst for CWPO. Application to chlorophenols. Appl Catal B 136–137:218–224

Munoz M, de Pedro ZM, Casas JA, Rodriguez JJ (2015) Preparation of magnetite-based catalysts and their application in heterogeneous Fenton oxidation—a review. Appl Catal B 176–177:249–265

Munoz M, Conde J, de Pedro ZM, Casas JA (2017a) Antibiotics abatement in synthetic and real aqueous matrices by H_2O_2/natural magnetite. Catal Today. https://doi.org/10.1016/j.cattod.2017.10.032

Munoz M, Domínguez P, de Pedro ZM, Casas JA, Rodriguez JJ (2017b) Naturally-occurring iron minerals as inexpensive catalysts for CWPO. Appl Catal B 203:166–173

Oliveira LCA, Fabris JD, Rios RRVA, Mussel WN, Lago RM (2004) $Fe_3{-}xMn_xO_4$ catalysts: phase transformations and carbon monoxide oxidation. Appl Catal B 259:253–259

Pereira MC, Oliveira LCA, Murad E (2012) Iron oxide catalysts: Fenton and Fenton-like reactions -a review. Clay Miner 47:285–302

Petrie B, Barden R, Kasprzyk-Hordern B (2015) A review on emerging contaminants in wastewaters and the environment: current knowledge, understudied areas and recommendations for future monitoring. Water Res 72:3–27

Pouran SR, Raman AAA, Daud WMAW (2014) Review on the application of modified iron oxides as heterogeneous catalysts in Fenton reactions. J Clean Prod 64:24–35

Ribeiro RS, Silva AMT, Figueiredo JL, Faria JL, Gomes HT (2016) Catalytic wet peroxide oxidation: a route towards the application of hybrid magnetic carbon nanocomposites for the degradation of organic pollutants. A review. Appl Catal B 187:428–460

Sandell EB (1959) Colorimetric determination of traces of metals. Interscience Pubs, New York

Souza WF, Guimaraes IR, Lima DQ, Silva CLT, Oliveira LCA (2009) Brazilian limonite for the oxidation of quinoline: high activity after a simple magnetic separation. Energy Fuel 23:4426–4430

Tang SCN, Lo IMC (2013) Magnetic nanoparticles: essential factors for sustainable environmental applications. Water Res 47:2613–2632

Tang J, Wang J (2018) Metal organic framework with coordinatively unsaturated sites as efficient Fenton-like catalyst for enhanced degradation of sulfamethazine. Environ Sci Technol. https://doi.org/10.1021/acs.est.8b00092

Tiernan MJ, Barnes PA, Parkes GMB (2001) Reduction of iron oxide catalysts: the investigation of kinetic parameters using rate perturbation and linear heating thermoanalytical techniques. J Phys Chem B 105:220–228

Vecchia ED, Coisson M, Appino C, Vinai F, Sethi R (2008) Magnetic characterization and interaction modelling of zerovalent iron nanoparticles for the remediation of contaminated aquifers. J Nanosci Nanotechnol 9:1–9

Verlicchi P, Galletti A, Petrovic M, Barceló D (2010) Hospital effluents as a source of emerging pollutants: an overview of micropollutants and sustainable treatment options. J Hydrol 389:416–428

Xu L, Wang J (2011) A heterogeneous Fenton-like system with nanoparticulate zero-valent iron for removal of 4-chloro-3-methyl phenol. J Hazard Mater 186:256–264

Yamashita T, Hayes P (2008) Analysis of XPS spectra of Fe^{2+} and Fe^{3+} ions in oxide materials. Appl Surf Sci 254:2441–2449

Zhang S, Zhao X, Niu H, Shi Y, Cai Y, Jiang G (2009) Superparamagnetic Fe_3O_4 nanoparticles as catalysts for the catalytic oxidation of phenolic and aniline compounds. J Hazard Mater 167:560–566

Zubir NA, Yacou C, Motuzas J, Zhang X, Diniz da Costa JC (2014) Structural and functional investigation of graphene oxide–Fe_3O_4 nanocomposites for the heterogeneous Fenton-like reaction. Sci Rep 4:1–8